FULL PAPER

Dalton
www.rsc.org/dalton

Dependence of the rotational barrier of the Ar-group in $RArTeX_2$ on the R-group [Ar = 2,6-$(MeO)_2C_6H_3$; R = Me, Et, *i*-Pr; X = Cl, Br, I]

Masahiro Asahara,* Shoichiro Taomoto, Masahito Tanaka, Tatsuo Erabi and Masanori Wada
Department of Materials Science, Faculty of Engineering, Tottori University, Koyama, Tottori, 680-8552, Japan

Received 11th October 2002, Accepted 8th January 2003
First published as an Advance Article on the web 30th January 2003

Alkyl(2,6-dimethoxyphenyl)tellurium dihalides, $RArTeX_2$ [Ar = 2,6-$(MeO)_2C_6H_3$; X = Cl **2a**–**c**, Br **3a**–**c**, I **4a**–**c**; R = Me **a**, Et **b**, *i*-Pr **c**] were prepared by the reactions of alkyl 2,6-dimethoxyphenyl telluride, RArTe **1**, with $SOCl_2$, Br_2 or I_2, respectively. The rotational barrier $\Delta G^{\ddagger}$ of the Ar-group around the Te–C bond in **2a**–**c**, **3a**–**c** and **4a**–**c** estimated by variable temperature ^{1}H NMR spectra was dependent on the alkyl (R) group as well as on the halogen atoms. It decreased in the order R = Me > Et > *i*-Pr as well as X = Cl > Br > I. The ^{125}Te resonances of **1** were observed at higher magnetic fields than those of RPhTe, and those of **1a–c**, **2a**–**c**, **3a**–**c** and **4a**–**c** shifted to lower magnetic field in the order R = Me > Et > *i*-Pr. The X-ray crystallographic analyses of **2a**–**c**, **3a**, **3b** and **4a** showed that the geometry around tellurium was pseudo-trigonal bipyramidal with the alkyl group, the Ar group and a lone pair of electrons in the equatorial positions and with two halogen atoms in the apical positions. Whereas each of the Te–C(Ar) bond distances were very similar [2.10 ± 0.01 Å], the Te–C(R) bonds of **2a**–**c** were longer than Te–C(Ar) and increased in length in the order R = Me < Et < *i*-Pr. The C(Ar)–Te–C(R) bond angles also increased in the order R = Me < Et < *i*-Pr. These molecules were bridged by intermolecular Te ··· X bonding to form dimers or polymers. Based on these results and VSEPR theory, the dependence of the rotational barrier $\Delta G^{\ddagger}$ of the Ar-group in $RArTeX_2$ on the R-group is discussed.

Valence shell electron-pair repulsion theory (VSEPR theory) predicts that the Te atom in diphenyltellurium dihalides, Ph_2TeX_2, in solutions is in a pseudo-trigonal bipyramidal coordination with two Te–C bonds and a lone pair of electrons occupying the equatorial sites and with two halogen atoms occupying the apical sites.[1] The actual shape of the molecule is like a seesaw form. The prediction has been supported by crystal structure analyses.[2–5] When the phenyl groups have substituents at 2,6-positions, the rotation of the phenyl group around the Te–C(Ar) bonds is restricted due to the barriers between the 2,6-substituents and the halogen atoms, as observed in the ^{1}H NMR studies of bis(2,6-dimethylphenyl)tellurium dihalides,[6] bis(2,6-dimethoxyphenyl)tellurium dihalides,[7] and bis(2,6-difluorophenyl)tellurium dihalides.[8] In these studies, the influence of the interaction between the two aryl groups on the rotational barrier is unknown. In addition, while crystal structure analyses of a variety of diaryltellurium dihalides have been reported, [2–15] few are known for alkyltellurium derivatives. In the present paper, we report the systematic investigation of alkyl(2,6-dimethoxyphenyl)tellurium dihalides, $RArTeX_2$ **2a**–**c**, **3a**–**c** and **4a**–**c** (see Scheme 1) by ^{1}H, ^{13}C and ^{125}Te NMR spectroscopy and X-ray crystal structure analyses. We also discuss the influence of an alkyl group at an equatorial position on the rotational barrier of the Te–C(Ar) bonds. During the course of our present investigation, we noticed fundamental errors in calculations of the rotational barrier$\Delta G^{\ddagger}$ in the previous paper.[7] It was calculated by applying equation (1),[16] but

$$\Delta G^{\ddagger}/(RT_c) = 22.96 + \log_e(T_c/\delta\nu) \qquad (1)$$

with an incorrect unit for $\delta\nu$ (ppm instead of Hz). Thus, we correct $\Delta G^{\ddagger}$ values for Ar_2TeX_2 **2d**–**5d** [Ar = 2,6-$(MeO)_2C_6H_3$; X = Cl **2**, Br **3**, I **4**, SCN **5**] as shown in Table 4 (later).

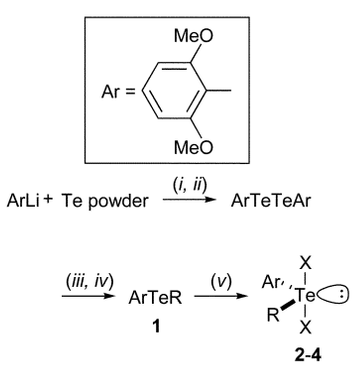

	R	X
2a	Me	Cl
2b	Et	Cl
2c	*i*-Pr	Cl
3a	Me	Br
3b	Et	Br
3c	*i*-Pr	Br
4a	Me	I
4b	Et	I
4c	*i*-Pr	I

Scheme 1 Reagents and conditions: (*i*) LiCl/THF, 0 °C~rt, 20 h; (*ii*) $+O_2$; (*iii*) $+NaBH_4$/EtOH; (*iv*) +RX, rt, 3 h; (*v*) $+SOCl_2$/toluene, $+Br_2$/EtOH, or $+I_2$/EtOH, rt, 0.5 h.

Experimental

General

^{1}H NMR spectra were recorded for solutions using a JEOL model JNM-GX270 spectrometer. ^{1}H chemical shifts were referenced to internal TMS (δ 0.00) in $CDCl_3$ or DMSO-d_6 (δ 2.49). ^{13}C and ^{125}Te NMR spectra were recorded for solutions in $CDCl_3$ using a JEOL model JNM-ECP500 spectrometer. ^{13}C NMR chemical shifts were referenced to internal $CDCl_3$ (δ 77.00), and ^{125}Te NMR chemical shifts were referenced to external diphenylditelluride (δ 450). The ^{1}H, ^{13}C, and ^{125}Te NMR spectral data are summarized in Tables 1 and 2. The preparations of ArTeTeAr, MeArTe **1a**, EtArTe **1b** and Ar_2TeX_2 **2d**–**5d** have been reported elsewhere.[7,17]

Preparation of isopropyl 2,6-dimethoxyphenyl telluride 1c

To a suspension of ArTeTeAr (2.6 g, 5 mmol) in ethanol (100 cm^3) was added $NaBH_4$ (0.63 g, 15 mmol) with stirring, followed by addition of 2-bromopropane (0.94 cm^3, 10 mmol). After stirring for 3 h, the reaction mixture was concentrated *in vacuo*, and water (100 cm^3) and chloroform (100 cm^3) were added for extraction. The chloroform layer was dried over anhydrous magnesium sulfate and was concentrated *in vacuo* to give a pale-brown liquid of **1c** in 86% yield. It was characterized by ^{1}H and ^{13}C NMR spectra. ^{1}H NMR (270 MHz, $CDCl_3$):

DOI: 10.1039/b210033a

Table 1 ^{1}H NMR spectral data for $RArTeX_2$ in $CDCl_3$ at 25 °C[a]

Compound	4-*H*[b]	3,5-*H*[c]	2,6-MeO-*H*[d]	-C*H*$_3$	Others
2a	7.43	6.66	3.95, 3.99	3.48[d] ($^2J_{Te-H}$= 33 Hz)	
2b	7.42	6.66, 6.65	3.93, 3.98	1.86[b] ($^3J_{Te-H}$ = 66 Hz)	4.12[f]
2c	7.42	6.66	3.93, 3.96[e]	1.90[c] ($^3J_{Te-H}$ = 48 Hz)	4.73[g]
3a	7.44	6.63	3.95, 4.00	3.61[d] ($^2J_{Te-H}$= 35 Hz)	
3b	7.43	6.64[e]	3.95, 3.99	1.83[b] ($^3J_{Te-H}$ = 65 Hz)	4.23[f]
3c	7.43	6.64	3.95[e]	1.93[c] ($^3J_{Te-H}$ = 45 Hz)	4.81[g]
4a	7.46	6.58	3.98	3.61[d] ($^2J_{Te-H}$= 33 Hz)	
4b	7.45	6.59	3.96	1.73[b] ($^3J_{Te-H}$ = 64 Hz)	4.18[f]
4c	7.45	6.59	3.96	1.96[c] ($^3J_{Te-H}$ = 40 Hz)	4.70[g]

[a] 270.17 MHz, δ/ppm, All J_{H-H} are 8 Hz. [b] A triplet. [c] A doublet. [d] A singlet. [e] Broad. [f] A quartet, -C*H*$_2$-. [g] A septet, ≡C*H*.

Table 2 ^{13}C NMR[a] and ^{125}Te NMR[b] spectral data for $RArTeX_2$ in $CDCl_3$ at 25 °C

	2,6-*C*	4-*C*	3,5-*C*	1-*C*	-O*C*H$_3$	Te*C*	TeC*C*	^{125}*Te*
2a	161.3, 159.3	134.7	106.0, 104.6	112.8	57.2, 56.2	26.8		794 (33)[d]
2b	160.6, 159.3	134.6	105.7, 104.6	114.0	57.1, 56.2	42.3	10.9	882 (66)[e]
2c	160.3, 159.9	134.6	105.6, 104.9	114.0	57.0, 56.0	53.9	21.2 (43)[c]	990 (48)[f]
3a	161.7, 159.4	134.7	106.0, 104.7	108.5	57.2, 56.3	25.5		717 (35)[d]
3b	161.1, 159.4	134.7	105.8, 104.7	109.9	57.1, 56.3	41.7	11.0	816 (65)[e]
3c	160.7, 160.0	134.7	105.6, 105.0	109.7	57.0, 56.0	52.4	21.8 (37)[c]	955 (45)[f]
4a	162.2, 159.3	134.5	106.1, 104.8	101.6	57.1, 56.2	23.2		602 (33)[d]
4b	161.5, 159.5	134.5	105.9, 105.0	103.3	57.0, 56.1	39.8	11.0	714 (64)[e]
4c	160.7	134.6	105.3	103.0	56.3	49.1	22.9 (33)[c]	901 (40)[f]

[a] 125.8 MHz, δ/ppm. [b] 157.9 MHz, δ/ppm. [c] $^3J_{TeC}$/Hz. [d] A quartet, $^2J_{TeH}$/Hz. [e] A quartet, $^3J_{TeH}$/Hz. [f] A septet, $^3J_{TeH}$/Hz.

δ 7.25 (t, J_{HH} = 8 Hz, 1H; 4-*H*), 6.53 (d, J_{HH} = 8 Hz, 2H; 3,5-*H*), 3.85 (s, 6H; 2,6-C*H*3O), 4.03 (septet, J_{HH} = 8 Hz, 1H; $(CH_3)_2$-C*H*-), 1.53 (dd, J_{HH} = 8 Hz, $^3J_{TeH}$ = 34 Hz, 6H; C*H*$_3$-); ^{13}C NMR (125.8 MHz, $CDCl_3$): δ 161.3, 129.9, 103.4, 93.5, 55.9, 26.1 (J_{TeC} = 36 Hz), 14.6 (J_{TeC} = 141 Hz); ^{125}Te NMR (157.9 MHz, $CDCl_3$): δ 455.

Preparations of alkyl(2,6-dimethoxyphenyl)tellurium dichlorides 2a–c

MeArTeCl$_2$ 2a. To a solution of **1a** (0.70 g, 2.5 mmol) in dry toluene (25 cm^3) was added SO_2Cl_2 (0.2 cm^3, 2.5 mmol) under an argon atmosphere, and the mixture was stirred vigorously for 0.5 h. The resultant precipitates were recrystallized from toluene/hexane to give white crystals of methyl(2,6-dimethoxyphenyl)tellurium dichloride, MeArTeCl$_2$ **2a** in 84% yield; mp (decomp.) 190–192 °C (Found: C, 30.75; H, 3.12%. $C_9H_{12}Cl_2O_2Te_1$ requires C, 30.82; H, 3.45%).

EtArTeCl$_2$ 2b. Using **1b** as above, EtArTeCl$_2$ **2b** was prepared in 80% yield as white crystals; mp 171–173 °C (Found: C, 32.88; H, 3.74%. $C_{10}H_{14}Cl_2O_2Te_1$ requires C, 32.93; H, 3.87%).

***i*-PrArTeCl$_2$ 2c.** Using **1c** as above, *i*-PrArTeCl$_2$ **2c** was prepared in 88% yield as white crystals; mp (decomp.) 189–192 °C (Found: C, 34.86; H, 4.11%. $C_{11}H_{16}Cl_2O_2Te_1$ requires C, 34.88; H, 4.26%).

Preparations of alkyl(2,6-dimethoxyphenyl)tellurium dibromides 3a–c

MeArTeBr$_2$ 3a. To a solution of **1a** (0.28 g, 1.0 mmol) in ethanol (6 cm^3) was added bromine (0.064 cm^3, 1.2 mmol). The mixture was stirred vigorously for 0.5 h to give pale yellow crystals of methyl(2,6-dimethoxyphenyl)tellurium dibromide, MeArTeBr$_2$ **3a** in 86% yield; mp (decomp.) 164 °C (Found: C, 24.54; H, 2.56%. $C_9H_{12}Br_2O_2Te_1$ requires C, 24.59; H, 2.75%).

EtArTeBr$_2$ 3b. Using **1b** as above, EtArTeBr$_2$ **3b** was prepared in 70% yield as pale yellow crystals; mp (decomp.) 156 °C (Found: C, 26.39; H, 2.89%. $C_{10}H_{14}Br_2O_2Te_1$ requires C, 26.48; H, 3.11%).

***i*-PrArTeBr$_2$ 3c.** Using **1c** as above, *i*-PrArTeBr$_2$ **3c** was prepared in 85% yield as pale yellow crystals; mp (decomp.) 135 °C (Found: C, 28.27; H, 3.25%. $C_{11}H_{16}Br_2O_2Te_1$ requires C, 28.25; H, 3.45%).

Preparations of alkyl(2,6-dimethoxyphenyl)tellurium diiodides 4a–c

MeArTeI$_2$ 4a. To a solution of **1a** (0.28 g, 1.0 mmol) in ethanol (6 cm^3) was added iodine (0.31 g, 1.2 mmol), and the mixture was stirred vigorously for 0.5 h. The resultant precipitates were filtered to give orange crystals of methyl(2,6-dimethoxyphenyl)tellurium diiodide, MeArTeI$_2$ **4a** in 83% yield; mp (decomp.) 131–140 °C (Found: C, 19.97; H, 2.08%. $C_9H_{12}I_2O_2Te_1$ requires C, 20.26; H, 2.27%).

EtArTeI$_2$ 4b. Using **1b** as above, EtArTeI$_2$ **4b** was prepared in 90% yield as orange crystals; mp (decomp.) 121 °C (Found: C, 21.87; H, 2.63%. $C_{10}H_{14}I_2O_2Te_1$ requires C, 21.93; H, 2.58%).

***i*-PrArTeI$_2$ 4c.** Using **1c** as above, *i*-PrArTeI$_2$ **4c** was prepared in 90% yield as orange crystals; mp (decomp.) 115 °C (Found: C, 23.47; H, 2.70%. $C_{11}H_{16}I_2O_2Te_1$ requires C, 23.52; H, 2.87%).

X-Ray crystallography

Single crystals of **2a**–**c**, **3a**,**b** and **4a** suitable for X-ray crystal structure analysis were obtained by recrystallization from nitromethane. The intensity data were collected at 173 K on a Rigaku RAXIS Rapid-S imaging plate area detector with graphite-monochromated MoKα (λ = 0.71070 Å) radiation. The data were corrected at a temperature of −100 ± 1 °C and for Lorentz and polarization effects. Their structures were solved by direct methods (SIR92)[18] and expanded using Fourier techniques (DIRDIF99).[19] The non-hydrogen atoms were refined anisotropically. Hydrogen atoms were included at calculated positions but not refined. All calculations were performed using the CrystalStructure crystallographic software package.[20,21] Their crystal data and experimental details are listed in Table 3.

CCDC reference numbers: 195252–195257.

Table 3 Crystal data and structure refinements for **2a–c**, **3a**,**b** and **4a**

	2a	**2b**	**2c**	**3a**	**3b**	**4a**
Empirical formula	$C_9H_{12}O_2Cl_2Te$	$C_{10}H_{14}O_2Cl_2Te$	$C_{11}H_{16}O_2Cl_2Te$	$C_9H_{12}O_2Br_2Te$	$C_{10}H_{14}O_2Br_2Te$	$C_9H_{12}O_2I_2Te$
Formula weight	350.70	364.73	378.75	439.60	453.63	533.60
Crystal size/mm^3	0.30 × 0.20 × 0.20	0.20 × 0.20 × 0.15	0.30 × 0.30 × 0.20	0.40 × 0.30 × 0.20	0.40 × 0.30 × 0.30	0.20 × 0.20 × 0.10
Crystal system	orthorhombic	orthorhombic	orthorhombic	orthorhombic	orthorhombic	monoclinic
Lattice parameters:						
a/Å	8.3486(1)	6.7317(2)	7.0124(4)	8.5520(1)	6.8905(2)	7.6021(4)
b/Å	13.6876(2)	15.2528(3)	15.1295(5)	13.6294(2)	15.5279(8)	11.5143(3)
c/Å	20.6906(3)	25.9327(5)	26.187(1)	21.2777(3)	26.0281(7)	15.5013(5)
β/°						92.204(2)
V/Å^3	2364.36(5)	2662.70(9)	2778.3(2)	2480.10(5)	2784.9(1)	1355.87(8)
Space group	*Pbca* (No. 61)	*Pbca* (No. 61)	*Pbca* (No. 61)	*Pbca* (No. 61)	*Pbca* (No. 61)	$P2_1/a$ (No. 14)
Z	8	8	8	8	8	4
D_{calcd}/g cm^{-3}	1.970	1.819	1.811	2.354	2.164	2.614
μ(MoKα)/cm^{-1}	29.41	26.15	25.10	88.37	78.74	67.27
$2\theta_{max}$/°	54.9	54.9	54.4	54.9	54.9	54.9
Reflections total	21625	23374	22671	20934	23541	11584
Observations ($I > -10\sigma(I)$)	2697	2542	3078	2816	3133	3069
No. of variables	139	150	161	139	150	140
*R*1, *wR*2	0.023, 0.087	0.020, 0.071	0.024, 0.108	0.023, 0.040	0.034, 0.132	0.028, 0.139
GOF	1.03	1.00	1.02	1.04	1.02	1.02

See http://www.rsc.org/suppdata/dt/b2/b210033a/ for crystallographic data in CIF or other electronic format.

Results

Preparation of alkyl(2,6-dimethoxyphenyl)tellurium dihalides, $RArTeX_2$

Alkyl 2,6-dimethoxyphenyl tellurides, RArTe **1a–c** were readily transformed into alkyl(2,6-dimethoxyphenyl)tellurium dihalides, $RArTeX_2$ **2a–c**, **3a–c** and **4a–c** by the reaction with $SOCl_2$, Br_2 or I_2, respectively, in 70–90% yields, as shown in Scheme 1. They were white (**2**), yellow (**3**) or orange (**4**) crystals with definite melting points at higher temperatures than 100 °C.

^{1}H, ^{13}C and ^{125}Te NMR spectra

The ^{1}H, ^{13}C and ^{125}Te NMR spectral data of **2–4** are summarized in Tables 1 (^{1}H) and 2 (^{13}C and ^{125}Te), respectively. As observed for Ar_2TeX_2 **2d–5d**,[7] the ^{1}H NMR spectra of **2a–c**, **3a–c** and **4a–c** were temperature-dependent (Fig. 1), indicating that the rotation of Te–C(Ar) bonds is restricted in solution. The coalescence temperatures, T_c, of **2a–c** in $CDCl_3$ were too high to be observed, but they could be observed for DMSO-d_6 solutions. Those of **3a–c** and **4a–c** could be observed for $CDCl_3$ solutions but not for DMSO-d_6 solutions due to the solidification at such low temperatures. We also failed to record the spectra of **2a–c**, **3a–c** and **4a–c** in D_2O due to their poor solubilities. From these T_c and the chemical shift difference $\delta\nu$, the rotational barriers $\Delta G^{\ddagger}$ of the Ar-group were calculated as summarized in Table 4, in which the corrected $\Delta G^{\ddagger}$ values of **2d–5d** are also given.

As observed for **2d–5d**, the rotational barriers $\Delta G^{\ddagger}$ of **2a–c**, **3a–c** and **4a–c** were also influenced by the halogen X, and decreased in the order X = Cl > Br > I. Although we could not calculate $\Delta G^{\ddagger}$ values for **3a–c** in $CDCl_3$, they must be larger in $CDCl_3$ than in DMSO-d_6.[7] A very interesting result obtained in the present study is that the $\Delta G^{\ddagger}$ values in **2a–c**, **3a–c** and **4a–c** were influenced also by the equatorial substituent R, and decreased in the order R = Me > Et > *i*-Pr, the reverse order of bulkiness. In order to obtain more information, the X-ray crystal structure analyses for some of the present compounds were performed (see below).

The ^{13}C NMR spectra of **2a–c**, **3a–c** and **4a–c**, except for **4c**, measured at 25 °C in $CDCl_3$ were consistent with the asymmetry of the 2,6-dimethoxyphenyl group, showing six nonequivalent resonances for the phenyl carbons and two nonequivalent resonances for the methoxy carbons. The

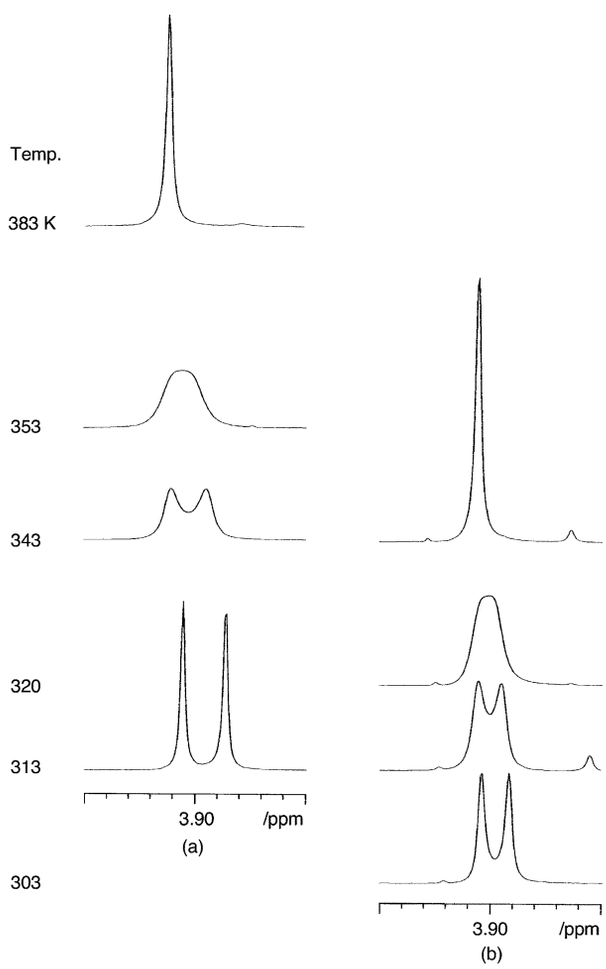

Fig. 1 Temperature-dependent ^{1}H NMR spectra of (a) **2a** and (b) **2c** in DMSO-d_6.

ipso-carbon resonance was quite sensitive to the changes of X, and shifted to higher magnetic field in the order X = Cl < Br < I. The Te–C(R) carbon resonance was observed at higher magnetic fields in the order Me > Et > *i*-Pr, and it also shifted to higher magnetic fields in the order X = Cl < Br < I. These ^{13}C resonances of **2a–c**, **3a–c** and **4a–c** were observed at lower magnetic fields than those of **1a–c**, respectively.

The ^{125}Te NMR spectra of RPhTe (R = Me, Et, *i*-Pr) in $CDCl_3$ have been reported, and the ^{125}Te resonance was

Table 4 Temperature-dependent ^{1}H NMR [a] data of $RArTeX_2$ **2**–**5**

	R	X	T_c/K	$\delta\nu$/Hz	$\Delta G^{\ddagger}$/kJ mol^{-1}
2a [b]	Me	Cl	353	10.0	78
2b [b]	Et	Cl	343	11.9	75
2c [b]	*i*-Pr	Cl	320	6.8	71
3a	Me	Br	328	13.2	71
3b	Et	Br	316	13.8	69
3c	*i*-Pr	Br	285	7.8	63
4a	Me	I	298	15.4	64
4b	Et	I	276	14.6	61
4c	*i*-Pr	I	235	3.0	53
2d [b]	Ar	Cl	360	96.7	73 [c]
3d [b]	Ar	Br	324	95.1	65 [c]
4d	Ar	I	244	88.1	49 [c]
5d	Ar	SCN	≥333	157.8	≥66 [c]

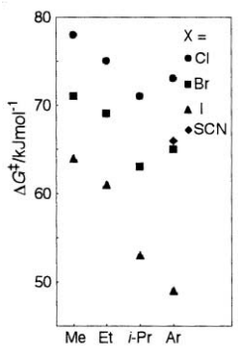

[a] 270.17 MHz in $CDCl_3$. [b] DMSO-d_6. [c] The corrected data for ref. 7 based on their $\delta\nu$ value.

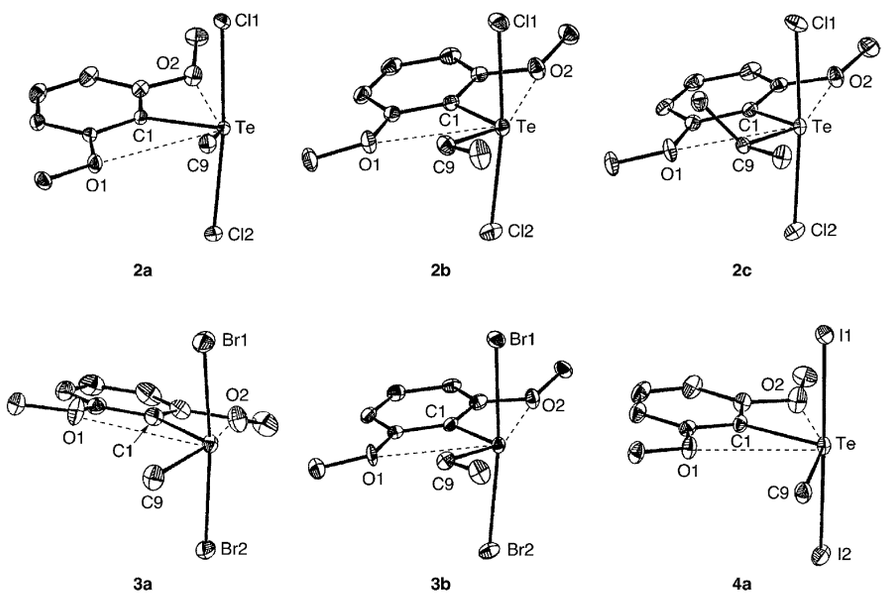

Fig. 2 X-Ray crystal structures of $RArTeX_2$ **2a**–**c**, **3a**,**b** and **4a** drawn at 30% probability level. All hydrogen atoms are omitted for clarity.

observed at lower magnetic fields in the order R = Me (δ +349) > Et (δ +552) > *i*-Pr (δ +720).[22] The ^{125}Te resonances of **1** were observed at higher magnetic fields [R = Me (δ +127), Et (δ +307), *i*-Pr (δ +455)] than those of RPhTe, indicating the possibility of an interaction of the 2,6-methoxy oxygen atoms with tellurium. The ^{125}Te resonances of **2a**–**c**, **3a**–**c** and **4a**–**c** were observed also at lower magnetic field in the order R= Me > Et > *i*-Pr, as observed for R_2TeCl_2.[23,24] The resonances were sensitive also to changes of X, and they shifted to the lower magnetic field in the order X = Cl < Br < I, as observed for Me_2TeX_2.[7,23,24] As reported for R_2TeBr_2 (R = Me, Et, *i*-Pr),[23] no coupling constant $^2J_{Te-H}$ could be observed for R = Et and *i*-Pr derivatives of **2a**–**c**, **3a**–**c** and **4a**–**c**, while $^3J_{Te-H}$ could be observed.

X-Ray crystal structures of some alkyl(2,6-dimethoxyphenyl)-tellurium dihalides

The molecular structures of **2a**–**c**, **3a**,**b** and **4a** are shown in Fig. 2, and their intermolecular relationships are shown in Fig. 3. The crystal data are listed in Table 3, and selected interatomic distances and angles are given in Table 5. The geometry around the tellurium atom of each compound is essentially pseudo-trigonal bipyramidal with one alkyl group (Me, Et or *i*-Pr), one Ar-group and a lone pair of electrons occupying the equatorial sites and with two halogen atoms occupying the apical sites. For comparison, selected bond distances and angles of reported compounds such as Me_2TeX_2,[25–27] Ph_2TeX_2[2,4,5] and Ar_2TeX_2 **2d**–**4d**[7] are given in Table 6.

Whereas each of the Te–C(Ar) bond distances are almost equal [2.091–2.109 Å] to those found for **2d**–**4d**,[7] the Te–C(R) bonds of **2a**–**c**, **3a**, **3b**, and **4a** were longer than the Te–C(Ar) bonds, and they increased remarkably in the order R = Me [2.111–2.123 Å] < Et [2.145, 2.149 Å] < *i*-Pr [2.178 Å].

The C–Te–C bond angles [101.9–108.0°] of **2a**–**c**, **3a**,**b** and **4a** are much smaller, as expected from VSEPR theory, than 120°, the ideal angle of trigonal bipyramidal geometry. The angles of the methyl derivatives **2a**, **3a**, **4a** [102.7, 101.9, 102.2°, respectively] are wider than those reported for Me_2TeX_2 [91–98°][25–27] and Ph_2TeX_2 [94–99°][2,4,5] but narrower than those reported for **2d**–**4d** [106.2–107.6°]. The C–Te–C bond angle of **2a**–**c** increases in the order R = Me < Et < *i*-Pr [102.7, 106.1, 108.0°, respectively], which is attributed tentatively to the steric effects of R-groups.

The two Te–X bond lengths in **2a**–**c**, **3a**,**b** and **4a** are not equivalent due probably to the intermolecular secondary bonding interaction (Fig. 3). The bond lengths [Te–Cl 2.483–2.559 Å, Te–Br 2.641–2.722 Å, Te–I 2.898, 2.935 Å] are in the range or somewhat longer than those reported for Me_2TeX_2, Ph_2TeX_2 and Ar_2TeX_2 [Te–Cl 2.480–2.541 Å, Te–Br 2.622–2.707 Å, Te–I 2.854–2.994 Å]. These molecules are bridged by intermolecular Te ··· X bonds to form dimers (**2a**–**c**, **3a**,**b**) or a polymer (**4a**). The intermolecular Te ··· X bonds in the dimers are located opposite to the Ar–Te bond. The intermolecular bond lengths

Table 5 Selected interatomic distances (Å) and angles (°) for **2a**–**c**, **3a**,**b** and **4a**

	2a (X = Cl)	**2b** (X = Cl)	**2c** (X = Cl)	**3a** (X = Br)	**3b** (X = Br)	**4a** (X = I)
Bond distances/Å						
Te–C1(Ar)	2.104(2)	2.098(2)	2.100(3)	2.109(3)	2.091(4)	2.109(3)
Te–C9(R)	2.111(3)	2.145(3)	2.178(3)	2.123(3)	2.149(5)	2.115(4)
Te–X1	2.559(1)	2.519(1)	2.488(1)	2.641	2.669(1)	2.935
Te–X2	2.483(1)	2.508(1)	2.532(1)	2.722	2.677(1)	2.898
Bond angles/°						
C1–Te–C9	102.7(1)	106.1(1)	108.0(1)	101.9(1)	106.2(2)	102.2(2)
X1–Te–X2	172.29(2)	172.12(2)	174.95(3)	174.23(1)	173.35(2)	178.77(1)
X1–Te–C1	87.48(7)	88.34(6)	88.00(8)	89.42(8)	87.8(1)	89.2(1)
X1–Te–C9	85.06(8)	88.49(7)	90.81(8)	90.9(1)	87.6(1)	90.4(1)
X2–Te–C1	88.32(7)	87.31(6)	88.25(8)	87.54(8)	89.0(1)	90.0(1)
X2–Te–C9	89.56(8)	86.41(7)	87.12(8)	85.0(1)	87.7(1)	88.8(1)
Interatomic distances/Å						
Te ··· O1	3.272(2)	3.223(2)	3.225(2)	3.271(2)	3.240(3)	3.318(3)
Te ··· O2	2.899(2)	2.909(2)	2.912(2)	2.886(2)	2.898(3)	2.853(3)
Te ··· X*	3.469(1)	3.617	3.823	3.558	3.716(1)	4.018
Te* ··· X	3.995(1)	3.617	3.823	4.114	3.716(1)	4.03
Te* ··· I**						4.018
Te** ··· I*						4.03

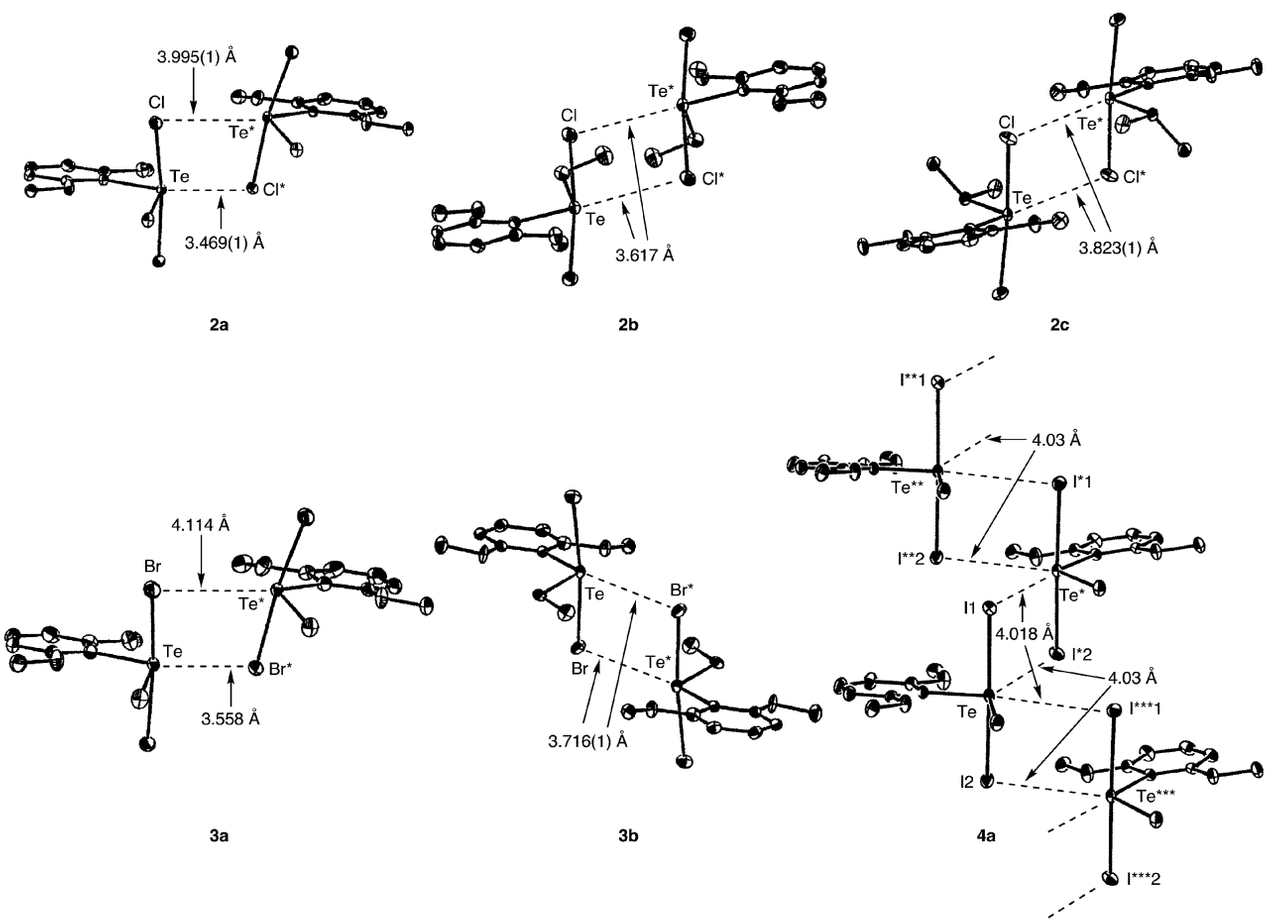

Fig. 3 Oligomeric structures of $RArTeX_2$ **2a**–**c**, **3a**,**b**, and **4a**.

are close to the sums of the van der Waals radii of Te and X: Te ··· Cl = 3.81 Å, Te ··· Br = 3.91 Å, and Te ··· I = 4.04 Å, respectively.[28] The presence of such intermolecular Te ··· X bonding has been observed for a variety of compounds of type R_2TeX_2.[2–6,8–13,25–27]

The X–Te–X bond angles in **2a**–**c**, **3a** and **4a** are very close to but slightly narrower than 180° as observed for Me_2TeX_2 and Ph_2TeX_2. The X–Te–X bonds are both bent slightly with the halogen atoms located closer between the alkyl and Ar groups, as expected from VSEPR theory.[4]

Discussion

A very interesting result obtained in the present study is that the rotational barrier $\Delta G^{\ddagger}$ of the Ar-group around the Te–C(Ar) bond in **2a**–**c**, **3a**–**c** and **4a**–**c** was influenced not only by the axial halogen atoms, X, but also by the equatorial substituent R, and it decreased in the orders X = Cl > Br > I and R = Me > Et > *i*-Pr, both the reverse orders of bulkiness. It seems necessary, however, to reconsider the precise causes of the rotational barrier $\Delta G^{\ddagger}$.

Table 6 Selected bond distances (Å) and angles (°) for R_2TeX_2

	Ar_2TeCl_2 **2d**[7]	Ar_2TeBr_2 **3d**[7]	Ar_2TeI_2 **4d**[7]
C(Ar)–Te	2.100(2)	2.092(3)	2.111(5)
Te–X	2.513(1)	2.6746(3)	2.9362(4)
C(Ar)–Te–C(Ar)	107.6(2)	107.5(2)	106.2(3)
X–Te–X	177.57(3)	179.36(1)	177.60(2)
	Me_2TeCl_2[25]	Me_2TeBr_2[27]	Me_2TeI_2[26]
C(Me)–Te	2.08(3), 2.10(3)	2.10(2), 2.22(2)	2.10(3)–2.16(3)
Te–X	2.480(10), 2.541(10)	2.622(3), 2.707(3)	2.854(3)–2.994(3)
C(Me)–Te–C(Me)	98.2(11)	97.4(8)	91(2)–97(2)
X–Te–X	172.3(3)	173.9(1)	177.3(2)–178.3(6)
	Ph_2TeCl_2[4]	Ph_2TeBr_2[2]	Ph_2TeI_2[5]
C(Ph)–Te	2.102(7), 2.111(7)	2.18(3)	2.122(15)–2.153(8)
Te–X	2.482(2), 2.529(3)	2.682(3)	2.883(1)–2.959(1)
C(Ph)–Te–C(Ph)	99.01(29)	93.9(12)	94.2(4)–96.7(5)
X–Te–X	175.54(7)	177.9(2)	174.23(4)–175.53(5)

The rotational barrier $\Delta G^{\ddagger}$ is the difference of the energies between the ground state and the transition state. The most probable conformations of these states are shown in Fig. 4, of which the transition state resembles an initial stage of the familiar Berry pseudo-rotation mechanism used to explain the exchange process between the equatorial halogens and the axial halogens in trigonal bipyramidal PX_5 molecules (X = F, Cl).[29] It is assumed for **2a–c**, **3a–c** and **4a–c** that, at the transition state, the X–Te–X sequence is bent with the halogen atoms located closer to both the lone pair electrons and the alkyl group to avoid the steric interaction between the Ar group and the X atoms. If the free rotation of the Ar-group in **2a–c**, **3a–c** and **4a–c** follows this process, the rotational barrier $\Delta G^{\ddagger}$ must be related to the difference of the total VSEPR energies between the ground state and such a transition state. At the transition state, the repulsion energy between the Ar–Te bonding electrons and the Te–X bonding electrons must decrease because of the increased Ar–Te–X angles, while the repulsion energies between the Te–X bonding electrons and both the lone pair electrons and the Te–C(R) bonding electrons must increase because of the decreased R–Te–X angles. The repulsion energy of **2a–c** at the transition state must be largest for **2a** because it has the shortest Te–C(R) bond among the three compounds, and the repulsion energy of **2c** must be the smallest because it has the longest Te–C(R) bond, as observed from the crystal structure analyses. Essentially in an analogous manner, the order of halogen influence may be explained, where the Te–X bonding electrons are located apart from the other electron pairs in the order X = Cl < Br < I.

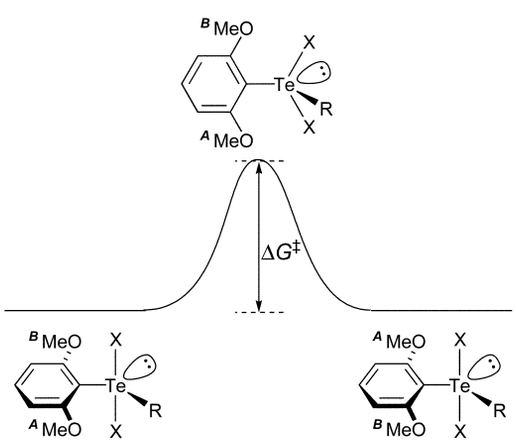

Fig. 4 Rotational barrier energy diagram.

In spite of the bulkiness of the Ar-group, the rotational barrier $\Delta G^{\ddagger}$ of **2d** was smaller than those of **2a** and **2b**, and that of **4d** was the smallest among the four iodides **4a–d** (Table 4). The Te–C(Ar) bonds were shorter than the Te–C(R) bonds. These results apparently are inconsistent with the explanation mentioned above. The true cause for the smaller $\Delta G^{\ddagger}$ of **2d–4d** than most of **2a–c**, **3a–c** and **4a–c** is unknown at present. It is worth noting here that the $\delta\nu$ values of **2d–4d** used for the calculation by equation (1) were much larger than those of **2a–c**, **3a–c** and **4a–c** (Table 4).

References

1 R. J. Gillespie and R. S. Nyholm, *Quart. Rev. Chem. Soc.*, 1957, **11**, 339; R. J. Gillespie, *J. Am. Chem. Soc.*, 1960, **82**, 5978; R. J. Gillespie, *Chem. Soc. Rev.*, 1992, **21**, 59.
2 G. D. Christofferson and J. D. McCullough, *Acta Crystallogr.*, 1958, **11**, 249.
3 F. J. Berry and A. J. Edwards, *J. Chem. Soc., Dalton Trans.*, 1980, 2306.
4 N. W. Alcock and W. D. Harrison, *J. Chem. Soc., Dalton Trans.*, 1982, 251.
5 N. W. Alcock and W. D. Harrison, *J. Chem. Soc., Dalton Trans.*, 1984, 869.
6 Y. Takaguchi, H. Fujihara and N. Furukawa, *J. Organomet. Chem.*, 1995, **498**, 49.
7 M. Asahara, M. Tanaka, T. Erabi and M. Wada, *J. Chem. Soc., Dalton Trans.*, 2000, 3493.
8 T. M. Klapötke, B. Krumm, P. Mayer, K. Polborn and O. P. Ruscitti, *Inorg. Chem.*, 2001, **40**, 5169.
9 G. Y. Chao and J. D. McCullough, *Acta Crystallogr.*, 1962, **15**, 887.
10 R. K. Chadha, J. E. Drake and M. A. Khan, *Acta Crystallogr., Sect. C*, 1983, **39**, 45.
11 R. H. Jones and T. A. Hamor, *J. Organomet. Chem.*, 1984, **262**, 151.
12 R. K. Chadha and J. E. Drake, *Acta Crystallogr., Sect. C*, 1984, **40**, 1349.
13 M. de Matheus, L. Torres, J. F. Piniella, J. L. Briansó and C. Miravitlles, *Acta Crystallogr., Sect. C*, 1991, **47**, 703.
14 Y. Wu, K. Ding, Y. Wang, Y. Zhu and L. Yang, *J. Organomet. Chem.*, 1994, **468**, 13.
15 E. S. Lang, R. M. Fernandes Jr., E. T. Silveira, U. Abram and E. M. Vázquez-López, *Z. Anorg. Allg. Chem.*, 1999, **625**, 1401.
16 R. J. Abraham, J. Fisher and P. Loftus, *Introduction to NMR Spectroscopy*, John Wiley & Sons, Chichester, Sussex, England, 1988.

17 M. Asahara, T. Morikawa, S.-i. Nobuki, T. Erabi and M. Wada, *J. Chem. Soc., Perkin Trans. 2*, 2001, 1899.
18 SIR92: A. Altomare, M. C. Burla, M. Camalli, M. Cascarano, C. Giacovazzo, A. Guagliardi and G. Polidori, *J. Appl. Crystallogr.*, 1994, **27**, 435.
19 DIRDIF99: P. T. Beurskens, G. Admiraal, G. Beurskens, W. P. Bosman, R. de Gelder, R. Israel and J. M. M. Smits, The DIRDIF-99 program system, Technical Report of Crystallography Laboratory, University of Nijmegen, The Netherlands, 1999.
20 CrystalStructure 2.00: Crystal Structure Analysis Package, Rigaku and MSC, Tokyo, Japan, 2001.
21 CRYSTALS Issue 10: D. J. Watkin, C. K. Prout, J. R. Carruthers and P. W. Betteridge, Chemical Crystallography Laboratory, Oxford, UK, 1996.
22 D. H. O'Brien, N. Dereu, C.-K. Huang, K. J. Irgolic and F. F. Knapp Jr., *Organometallics*, 1983, **2**, 305.
23 H. C. E. McFarlane and W. McFarlane, *J. Chem. Soc., Dalton Trans.*, 1973, 2416.
24 J. H. E. Bailey, J. E. Drake, L. N. Khasrou and J. Yang, *Inorg. Chem.*, 1995, **34**, 124.
25 G. D. Christofferson, R. A. Sparks and J. D. McCullough, *Acta Crystallogr.*, 1958, **11**, 782.
26 L. Y. Y. Chan and F. W. B. Einstein, *J. Chem. Soc., Dalton Trans.*, 1972, 316.
27 J. E. Drake, L. N. Khasrou, A. G. Mislankar and R. Ratnani, *Inorg. Chem.*, 1999, **38**, 3994.
28 A. Bondi, *J. Phys. Chem.*, 1964, **68**, 441.
29 R. S. Berry, *J. Chem. Phys.*, 1960, **32**, 933.